Polaronic electron transfer in β-sheet protein models

2001 J. Phys.: Condens. Matter 13 9821

(http://iopscience.iop.org/0953-8984/13/43/312)

INSTITUTE OF PHYSICS PUBLISHING JOURNAL OF PHYSICS: CONDENSED MATTER

J. Phys.: Condens. Matter **13** (2001) 9821–9834 PII: S0953-8984(01)27531-6

Polaronic electron transfer in β-sheet protein models

N K Voulgarakis[1,2], D Hennig[1,2], H Gabriel[2] and G P Tsironis[1]

[1] Physics Department, University of Crete, and Foundation for Research and Technology, Hellas, PO Box 2208, Heraklion 71003, Crete, Greece
[2] Freie Universität Berlin, Fachbereich Physik, Institut für Theoretische Physik, Arnimallee 14, 14195 Berlin, Germany

Received 2 August 2001
Published 12 October 2001
Online at stacks.iop.org/JPhysCM/13/9821

Abstract

We consider electron transfer (ET) along β-sheet forms of proteins. The secondary structure of the β-sheet proteins is modelled by a two-dimensional oscillator network whose constituents represent peptide units. Covalent and hydrogen bonds between the peptide units are represented by point–point interaction potentials. Intrapeptide vibrational degrees of freedom are taken into account by means of harmonic oscillators while the electronic motion is described within the framework of a tight-binding system. We construct polarons as stationary localized solution states utilizing a non-linear map approach. The polaron state represents a self-trapped electron in conjunction with its intrapeptide deformation field and the static deformation of the protein scaffolding. Furthermore, in the dynamical study we focus attention on the initiation of polaron motion, utilizing its pinning modes. We show that both the covalent and the hydrogen channel provide a path for coherent ET in β-sheet proteins. It is demonstrated that the interplay of the vibrations of the protein scaffolding and the electron dynamics promotes long-lived localized excitation patterns travelling coherently along the lattice of peptide units.

1. Introduction

The history of studies of energy storage and transport in biomacromolecules begins with the work of Landau [1] and Pekar [2] on self-trapped states. They introduced the concept of a polaron, i.e. an electron accompanied by its own lattice deformation forming a localized quasiparticle compound. Davydov showed that, when the size of the polaron is large enough that the continuum approximation can be applied to the underlying lattice system, a mobile self-trapped state can travel as a solitary wave along the molecular structure [3, 4]. Since the work of Davydov in the 1970s the relevance of solitons and/or polarons to the energy and particle transport in biomolecules has been recognized and has remained of great interest (see e.g. [5–7]). Most of the studies of transport properties in biomacromolecules have been based on one-dimensional non-linear lattice models, and recent two- and three-dimensional

extensions in relation to solitonic transport of vibrational energy can be found e.g. in [8–10]. The theory of the soliton-like ET mechanism in one-dimensional chain models of proteins is described in [4, 7]. Recently, it was proposed that supersonic acoustic solitons can capture and transfer self-trapping modes in anharmonic one-dimensional lattices [11]. As regards the enforcing role played by soliton motion in the functional processes in biomolecules, we note that in recent work it has been proposed that the folding and formation process of proteins may be mediated by solitons travelling along the polypeptide chains, while interacting with a field corresponding to the conformation angles of the protein [12]. Furthermore, in a non-linear dynamics approach to DNA dynamics it has been suggested that solitons propagating along the DNA molecule may play an important role in the denaturation and transcription process [13–15].

In the present work we study the transfer of an electron along the β-sheet secondary structure of proteins on the basis of the concepts of breathers and polarons. The secondary protein structure is modelled by a two-dimensional network of coupled oscillators, each element of it representing a peptide group. The peptide units are connected via point–point pair potentials modelling the covalent- and hydrogen-bond interactions. The electronic system is described by a tight-binding lattice. It is assumed that each peptide unit possesses one internal (intramolecular) vibrational degree of freedom represented e.g. by the C=O stretching mode. As will be shown, mutual couplings between (i) the electron amplitude and (ii) the intramolecular and intermolecular vibrations may lead to polaron formation.

The first part of the paper is devoted to the study of the stationary problem. We construct localized solutions of the combined electron–vibration system. In order to accomplish this we first derive a generalized discrete non-linear Schrödinger (DNLS) equation for the electronic amplitude and exploit a non-linear map approach to construct standing electronic breather solutions. The stationary electronic breather pattern having been obtained, the bond deformations attributed to the polaronic ground state of the complete system can be deduced. Thereafter, we perform a normal-mode analysis for the polarons to identify their pinning modes. The latter are then appropriately excited to initiate the mobility of a polaron. We demonstrate that the formation of soliton-like bond vibrations in coexistence with a moving electron breather provides long-lived coherent ET. Finally, in section 6 we give a summary of our results.

2. The β-sheet protein model

We consider the transfer of an electron along combined polypeptide chains encountered in secondary-structure forms of peptides. The most common secondary structures are helices consisting of folded peptide chains and β-sheets formed by combined β-strands. In the latter case, the protein backbone is as extended as possible, yielding a β-strand, and β-sheets are formed when two or more β-strands are located next to each other allowing for hydrogen bondings between the amide (NH) and carbonyl (CO) groups in the protein backbones [16–18]. References [19, 20] are devoted to the design of peptides adopting a β-sheet structure as well as the creation of native-like globular *de novo* proteins. Experimentally, solutions of identical synthetic *de novo* peptide molecules are used, which self-assemble into long β-sheet tape structures due to intermolecular hydrogen bonds [21, 22]. The secondary structure is determined by regular arrangements of the peptide units as well as the hydrogen bonds, i.e. all peptide units are aligned and connected in the same way.

Within our two-dimensional model of an aggregate of combined β-strands, the peptide groups are treated as single mass entities, whose equilibrium positions are assigned to the sites of a two-dimensional (non-square) lattice labelled by a pair of indices (n, μ). The index n

runs in the horizontal direction (the x-direction) along the sites (peptide groups) of a particular strand specified by μ which enumerates the strands vertically (in the y-direction). The bond interactions between the peptide groups hold the β-sheet in its stable secondary structure. Nearest-neighbour units on a strand located at (n, μ) and $(n \pm 1, \mu)$ are covalently linked. Peptide groups of different strands oppositely situated at (n, μ) and $(n, \mu \pm 1)$ are connected through hydrogen bonds. The covalent (hydrogen) bonds are highly directional parallel to the x-axis (y-axis), so we take only the displacements of the peptide groups in the x–y direction into account and discard any motion in the z-direction. The two-dimensional peptide backbone of a β-sheet is sketched in figure 1.

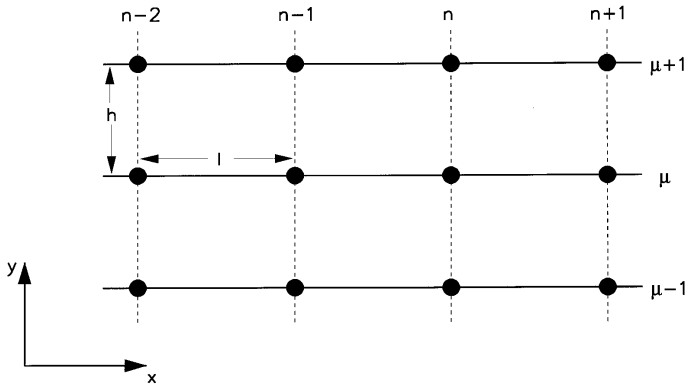

Figure 1. The two-dimensional structure of the β-sheet protein. The bullets representing the peptide units are horizontally (vertically) linked by covalent (hydrogen) bonds as sketched by full (dashed) lines.

Since the strong covalent bonds (bond energies of the order of 50–250 kcal mol^{-1}) are rather rigid compared to the comparatively weak and flexible H bonds (bond energies 1–7 kcal mol^{-1}) [18], it is reasonable to model the (small) distortions of the covalent bonds in a harmonic fashion. The vibrational dynamics of the elastic hydrogen bonds is treated anharmonically [23] by using Morse potentials. The Hamiltonian of the intermolecular interactions is given by

$$H_{inter} = \frac{1}{2m}\sum_n\sum_\mu p_{n\mu}^2 + \sum_n\sum_\mu U_{cov}(r_{n\mu}) + U_{hyd}(q_{n\mu})$$
$$= \frac{1}{2m}\sum_n\sum_\mu p_{n\mu}^2 + \frac{1}{2}\alpha\sum_n\sum_\mu r_{n\mu}^2 + \frac{1}{2}D\sum_n\sum_\mu(1-\exp[-aq_{n\mu}])^2 \qquad (1)$$

with the momentum vector $p_{n\mu} = (p_{n\mu}^{(x)}, p_{n\mu}^{(y)})$ associated with the displacements $(x_{n\mu}, y_{n\mu})$ of the peptide units from their equilibrium positions $(x_{n\mu}^{(0)}, y_{n\mu}^{(0)})$. The deviations of the covalent- and hydrogen-bond lengths from their equilibrium lengths l and h, respectively, are expressed as

$$r_{n\mu} + l = \left[(l + x_{n\mu} - x_{n-1,\mu})^2 + (y_{n\mu} - y_{n-1,\mu})^2\right]^{1/2} \qquad (2)$$

$$q_{n\mu} + h = \left[(x_{n\mu} - x_{n\mu-1})^2 + (h + y_{n\mu} - y_{n,\mu-1})^2\right]^{1/2}. \qquad (3)$$

In (1) the parameter α regulates the stiffness of the covalent bonds, m is the mass of a single peptide unit, D determines the break-up energy of the hydrogen bond and a is the range parameter of the Morse potential. The point–point intermolecular interaction potentials, are normalized to $U_{cov}(0) = U_{hyd}(0) = 0$ and $U'_{cov}(0) = U'_{hyd}(0) = 0$. Although the dynamics

of the modulation of the covalent bonds evolves in harmonic potentials, the corresponding dynamical equations are nonetheless non-linear due to the relation given as equation (2). The assumption that the lattice vibrations can be treated classically is tantamount to invoking a relatively strong coupling between the electron and the lattice vibrations.

For the ET the electronic part of the Hamiltonian is given by

$$H_e = \sum_n \sum_\mu \epsilon_{n\mu} |c_{n\mu}|^2 - \sum_n \sum_\mu W(q_{n\mu}) \left[c^*_{n\mu} c_{n,\mu-1} + c_{n\mu} c^*_{n,\mu-1} \right] - \sum_n \sum_\mu V(r_{n\mu}) \left[c^*_{n\mu} c_{n-1,\mu} + c_{n\mu} c^*_{n-1,\mu} \right] \tag{4}$$

where $c_{n\mu}$ represents the probability amplitude of the electron for occupation of the molecular site n on the strand of index μ and $\epsilon_{n\mu}$ is the on-site energy. The parameter $W(q_{n\mu})$ determines the interchain transfer matrix element providing vertical ET between hydrogen-bonded peptide units. The parameter $V(r_{n\mu})$ is the intrachain transfer matrix element enabling horizontal ET from one peptide unit to the neighbouring ones on a β-strand of index μ.

The local part of the vibrational Hamiltonian models an intramolecular (intrapeptide) vibrational degree of freedom, constituted e.g. by the amide-I vibrations of each of the peptide units. The dynamics of the intramolecular vibrations is simulated by a set of classical harmonic oscillators situated at sites (n, μ):

$$H_{intra} = \sum_{n\mu} \frac{1}{2M} P^2_{n\mu} + \frac{M\omega_0^2}{2} \sum_n Q^2_{n\mu} \tag{5}$$

with $P_{n\mu}$ and $Q_{n\mu}$ being the momentum and coordinate, respectively, corresponding to the displacement of an oscillator from its equilibrium position. M is the reduced mass and ω_0 the frequency.

The diagonal coupling between the electronic degree of freedom and the harmonic oscillators contained in the interaction Hamiltonian

$$H_{e-intra} = \kappa \sum_{n\mu} Q_{n\mu} |c_{n\mu}|^2 \tag{6}$$

takes vibrational modulations of the local electronic on-site energy $\epsilon_{n\mu} = \epsilon_0 + \kappa Q_{n\mu}$ into account and k is the electron–vibration coupling parameter.

The transfer matrix elements, whose values are determined by an overlap integral, are assumed to depend exponentially on the distances between the peptide units, which amount to

$$V(r_{n\mu}) = V_0 \exp[-b r_{n\mu}] \tag{7}$$

$$W(q_{n\mu}) = W_0 \exp[-d q_{n\mu}] \tag{8}$$

with the coupling parameters b and d. It is through equations (7) and (8) that the couplings between the electronic and bond vibrational degrees of freedom (d.o.f.) are introduced.

Finally, the interaction between the intramolecular and intermolecular vibrations is accounted for by

$$H_{intra-inter} = \sum_n \sum_\mu Q_{n\mu} \left[\beta_l (r_{n+1,\mu} + r_{n\mu}) + \beta_t (q_{n,\mu+1} + q_{n\mu}) \right] \tag{9}$$

which couples each local intramolecular vibrational coordinate $Q_{n\mu}$ with the bond coordinates $r_{n\mu}$ and $q_{n\mu}$. The coupling constants are denoted by β_t and β_l.

Altogether the total Hamiltonian of our model includes exchange between electronic, intramolecular and intermolecular vibrational energies.

We scale the time according to $\tilde{t} = \omega_0 t$ and introduce the dimensionless quantities

$$\tilde{W} = \frac{W_0}{V_0} \qquad \tilde{D} = \frac{D}{V_0} \qquad \tilde{Q}_{n\mu} = \sqrt{\frac{M\omega_0^2}{V_0}}\,Q_{n\mu} \qquad \tilde{P}_{n\mu} = \sqrt{\frac{M\omega_0^2}{V_0}}\,P_{n\mu}$$

$$\tilde{x}_{n\mu} = \sqrt{\frac{M\omega_0^2}{\lambda V_0}}\,x_{n\mu} \qquad (x_{n\mu} \longleftrightarrow y_{n\mu})$$

$$\tilde{p}^{(x)}_{n\mu} = \sqrt{\frac{\lambda}{MV_0}}\,p^{(x)}_{n\mu} \qquad (p^{(x)}_{n\mu} \longleftrightarrow p^{(y)}_{n\mu}) \tag{10}$$

$$\tilde{a} = \sqrt{\frac{V_0\lambda}{M\omega_0^2}}\,a \qquad (a \longleftrightarrow b, d)$$

$$\tilde{\beta}_{h,l} = \frac{\sqrt{\lambda}}{\omega_0^2 M}\beta_{h,l} \qquad \tilde{\kappa} = \frac{1}{\sqrt{V_0 M\omega_0^2}}\kappa$$

with the mass ratio $\lambda = M/m$. Now, to simplify the notation, the tildes are dropped. The corresponding scaled coupled equations of motion become

$$\begin{aligned}\mathrm{i}\gamma\dot{c}_{n\mu} = {} & \kappa Q_{n\mu}c_{n\mu} - W\exp(-dq_{n\mu})c_{n,\mu-1} - W\exp(-dq_{n,\mu+1})c_{n+1,\mu} \\ & - (\exp(-br_{n\mu})c_{n-1,\mu} + \exp(-br_{n+1,\mu})c_{n+1,\mu})\end{aligned} \tag{11}$$

$$\dot{P}_{n\mu} = -Q_{n\mu} - \kappa|c_{n\mu}|^2 - \beta_l(r_{n+1,\mu} + r_{n\mu}) - \beta_t(q_{n,\mu+1} + q_{n\mu}) \tag{12}$$

$$\dot{Q}_{n\mu} = P_{n\mu} \tag{13}$$

$$\begin{aligned}\dot{p}^{(x)}_{n\mu} = {} & \{-\alpha r_{n\mu} - \beta_l Q_{n\mu} - b[c^*_{n\mu}c_{n-1,\mu} + c_{n\mu}c^*_{n-1,\mu}]\}\frac{\partial r_{n\mu}}{\partial x_{n\mu}} \\ & - \{\alpha r_{n+1,\mu} + \beta_l Q_{n\mu} + b[c^*_{n\mu}c_{n+1,\mu} + c_{n\mu}c^*_{n+1,\mu}]\}\frac{\partial r_{n+1,\mu}}{\partial x_{n\mu}} \\ & - \{\beta_t Q_{n\mu} + dW\exp(-dq_{n\mu})[c^*_{n,\mu}c_{n\mu-1} + c_{n\mu}c^*_{n,\mu-1}] \\ & + aD(1 - \exp(-aq_{n\mu}))\exp(-aq_{n\mu})\}\frac{\partial q_{n\mu}}{\partial x_{n\mu}} \\ & - \{\beta_t Q_{n\mu} + dW\exp(-dq_{n,\mu+1})[c^*_{n,\mu+1}c_{n\mu} + c_{n,\mu+1}c^*_{n\mu}] \\ & + aD(1 - \exp(-aq_{n,\mu+1}))\exp(-aq_{n,\mu+1})\}\frac{\partial q_{n,\mu+1}}{\partial x_{n\mu}}\end{aligned} \tag{14}$$

$$\dot{x}_{n\mu} = p^{(x)}_{n\mu} \tag{15}$$

$$\begin{aligned}\dot{p}^{(y)}_{n\mu} = {} & \{-\alpha r_{n\mu} - \beta_l Q_{n\mu} - b[c^*_{n\mu}c_{n-1,\mu} + c_{n\mu}c^*_{n-1,\mu}]\}\frac{\partial r_{n\mu}}{\partial y_{n\mu}} \\ & - \{\alpha r_{n+1,\mu} + \beta_l Q_{n\mu} + b[c^*_{n\mu}c_{n+1,\mu} + c_{n\mu}c^*_{n+1,\mu}]\}\frac{\partial r_{n+1,\mu}}{\partial y_{n\mu}} \\ & - \{\beta_t Q_{n\mu} + dW\exp(-dq_{n\mu})[c^*_{n\mu}c_{n\mu-1} + c_{n,\mu}c^*_{n,\mu-1}] \\ & + aD(1 - \exp(-aq_{n\mu}))\exp(-aq_{n\mu})\}\frac{\partial q_{n\mu}}{\partial y_{n\mu}} \\ & - \{\beta_t Q_{n\mu} + dW\exp(-dq_{n,\mu+1})[c^*_{n,\mu+1}c_{n\mu} + c_{n,\mu+1}c^*_{n\mu}] \\ & + aD(1 - \exp(-aq_{n,\mu+1}))\exp(-aq_{n,\mu+1})\}\frac{\partial q_{n,\mu+1}}{\partial y_{n\mu}}\end{aligned} \tag{16}$$

$$\dot{y}_{n\mu} = p^{(y)}_{n\mu} \tag{17}$$

with

$$\frac{\partial r_{n\mu}}{\partial x_{n\mu}} = \frac{l + x_{n\mu} - x_{n-1,\mu}}{l + r_{n\mu}} \qquad \frac{\partial r_{n\mu}}{\partial y_{n\mu}} = \frac{y_{n\mu} - y_{n-1,\mu}}{l + r_{n\mu}} \tag{18}$$

$$\frac{\partial q_{n\mu}}{\partial x_{n\mu}} = \frac{x_{n\mu} - x_{n,\mu-1}}{l + q_{n\mu}} \qquad \frac{\partial q_{n\mu}}{\partial y_{n\mu}} = \frac{h + y_{n\mu} - y_{n,\mu-1}}{h + q_{n\mu}}. \tag{19}$$

The (small) value of the adiabaticity parameter $\gamma = \hbar\omega_0/V_0$ expresses the timescale separation between the fast intramolecular vibrations and the slow intermolecular ET. Through a simple phase transformation $\tilde{c}_n(t) = c_n(t)\exp[-\mathrm{i}\epsilon_0 t]$ we remove the term proportional to ϵ_0 from the electronic equation of motion. Furthermore, we approximate the distance dependence of the horizontal transfer matrix element as

$$V(r_{n\mu}) = V_0 \exp[-br_{n\mu}] \backsimeq V_0(1 - br_{n\mu}).$$

We remark that in the limit of $b = d = \beta_t = \beta_l = 0$ the intermolecular vibrations decouple from the electronic and intramolecular degrees of freedom and the reduced system can be viewed as a multi-strand extension of the standard (one-dimensional) Holstein model [24–26] with anisotropic longitudinal and transverse transfer matrix elements V and W. Moreover, the one-dimensional standard Holstein system is recovered in the limit $W = 0$.

In this study we use realistic parameter values for proteins [4, 7, 16]: $V \simeq 2.5$ eV, $W \leqslant 1.0$ eV, $D = 0.04$–0.3 eV, $m \simeq 100\, m_{proton}$, $\omega_0 = 3.11 \times 10^{14}$ s^{-1}, $a \approx b \approx d =$ 1–2 Å^{-1}, $\alpha = 0.96$–4.82 eV Å^{-2} and $\beta_l \backsimeq \beta_t \simeq 40 \times 10^{-3}$ eV Å^{-2}. The geometry of the β-sheet is characterized by typical horizontal distances $h = 2.75$ Å and vertical distances $l = 3.3$ Å.

3. Stationary solutions and polarons

In the following we construct polaron solutions of the coupled system describing the interaction of the electron with the intramolecular vibrations as well as the intermolecular bond oscillators.

To obtain polaron states of the β-sheet system we consider the corresponding stationary system for which $\dot{P}_{n\mu} = \dot{p}^{(x)}_{n\mu} = \dot{p}^{(y)}_{n\mu} = 0$ must hold and the real time-independent stationary electronic amplitude $\Phi_{n\mu}$ is determined by the relation $c_{n\mu} = \Phi_{n\mu}\exp(-\mathrm{i}Et/\gamma)$. Applied to equation (12), the stationarity condition leads to the instantaneous distortion

$$Q_{n\mu} = -\kappa|\Phi_{n\mu}|^2 - \beta_l(r_{n+1,\mu} + r_{n\mu}) - \beta_t(q_{n+1,\mu} + q_{n,\mu}) \tag{20}$$

which reduces to

$$Q_{n\mu} \simeq -\kappa|\Phi_{n\mu}|^2 \tag{21}$$

for weak-coupling parameters β_l and β_t.

Notice that in order to solve the stationary equations of the non-linear system of equations (11)–(15) we need to know both the stationary electronic pattern and the stationary deformations of all the bonds. To tackle the complete stationary system we first examine a simpler case by using the approximation (21) and neglect the low-energy hydrogen-bond terms of the total Hamiltonian, i.e. we set $D = d = 0$. For vanishing momenta $\dot{p}^{(x)}_{n\mu} = \dot{p}^{(y)}_{n\mu} = 0$,

$$\alpha\left(r_{n\mu}\frac{\partial r_{n\mu}}{\partial x_{n\mu}} + r_{n+1,\mu}\frac{\partial r_{n+1,\mu}}{\partial x_{n\mu}}\right) = -2b\left(\frac{\partial r_{n\mu}}{\partial x_{n\mu}}\Phi_{n\mu}\Phi_{n-1,\mu} + \frac{\partial r_{n+1,\mu}}{\partial x_{n\mu}}\Phi_{n\mu}\Phi_{n+1,\mu}\right) \tag{22}$$

and

$$\alpha\left(r_{n\mu}\frac{\partial r_{n\mu}}{\partial y_{n\mu}} + r_{n+1,\mu}\frac{\partial r_{n+1,\mu}}{\partial y_{n\mu}}\right) = -2b\left(\frac{\partial r_{n\mu}}{\partial y_{n\mu}}\Phi_{n\mu}\Phi_{n-1,\mu} + \frac{\partial r_{n+1,\mu}}{\partial y_{n\mu}}\Phi_{n\mu}\Phi_{n+1,\mu}\right) \tag{23}$$

must hold. Both equations (22) and (23) are satisfied if the distortions of the covalent bonds satisfy the condition

$$r_{n\mu} = -\frac{2b}{\alpha}\Phi_{n\mu}\Phi_{n-1,\mu}. \tag{24}$$

Hence, combining (21), (24) and the stationary equation for the electronic amplitude $\Phi_{n\mu}$ we end up with the following modified DNLS equation:

$$E\Phi_{n\mu} = -\left(1 + \frac{2b^2}{a}\Phi_{n\mu}\Phi_{n-1,\mu}\right)\Phi_{n-1,\mu} - \left(1 + \frac{2b^2}{a}\Phi_{n\mu}\Phi_{n+1,\mu}\right)\Phi_{n+1,\mu} - W_0(\Phi_{n,\mu-1} + \Phi_{n,\mu+1}) - \kappa^2|\Phi_{n\mu}|^2\Phi_{n\mu}. \tag{25}$$

The above equation is the exact DNLS equation for a two-dimensional (standard) polaron system. We can find the (electronic) ground state of equation (25) by using the numerical method outlined in reference [27]. To this end one exploits the fact that polarons (localized electronic states in conjuntion with vibrational displacements localized in the same lattice region) are obtained as the attractors of the map

$$\{\Phi\} \to \{\bar{\Phi}\} = H\{\Phi\}/||H\{\Phi\}|| \tag{26}$$

with

$$\{\Phi\} = \begin{pmatrix} \Phi_{1,\mu=1}, \Phi_{2,\mu=1}, \ldots, \Phi_{N,\mu=1} \\ \Phi_{1,\mu=2}, \Phi_{2,\mu=2}, \ldots, \Phi_{N,\mu=2} \\ \cdot \\ \cdot \\ \cdot \\ \Phi_{1,\mu=M}, \Phi_{2,\mu=M}, \ldots, \Phi_{N,\mu=M} \end{pmatrix} \tag{27}$$

where the operator H is determined by the r.h.s. of equation (26) and the norm of the state $H\{\Phi\}$ is defined [27] as

$$||H\{\Phi\}|| = \sqrt{\sum_{n\mu}(H\{\Phi\})^2}.$$

M determines the number of strands contained in the two-dimensional β-sheet configuration.

Note that in the limit of $b^2/a \to 0$ we obtain the expected DNLS equation for an anisotropic two-dimensional system. The ground state in the case of $d \neq 0$ and $D \neq 0$ is obtained by using the ground state of the (reduced) equation (25) as the initial condition for the complete system of equations of motion and invoking the relaxation concept. The latter is based on the reasonable assumption that the instantaneous distortions given by equation (21) are in close proximity to the genuine ground-state solution in configuration space. To reach the real (genuine) ground state we add a small damping term to each of equations (12), (14) and (16), and integrate numerically the complete β-sheet system of equations (11)–(15) using the following initial conditions:

$$\left\{\Phi_{n\mu}, 0, Q^{(0)}_{n\mu}, 0, x^{(0)}_{n\mu}, 0, y^{(0)}_{n\mu}, 0\right\} \tag{28}$$

where $Q^{(0)}_{n\mu}$ and $\Phi_{n\mu}$ are determined by equations (21) and (26), respectively. To initialize $x_{n\mu}$ and $y_{n\mu}$ we choose the elongations $r_{n,\mu}$ to be directed exclusively parallel to the x-axis (i.e. $r_{n,\mu} = (x_{n,\mu} - x_{n-1,\mu})$). Therefore one gets the initial values

$$x^{(0)}_{n\mu} - x^{(0)}_{n-1,\mu} = -\frac{2b}{\alpha}\Phi_{n\mu}\Phi_{n-1,\mu}$$

and

$$y^{(0)}_{n\mu} - y^{(0)}_{n-1,\mu} = 0.$$

After short integration times the system relaxes to the ground-state solution, i.e. the real stationary solution of the full non-linear system.

In figure 2 we display for the simplest β-sheet configuration, namely a two-strand ladder system, the localized patterns associated with the polaronic components of the electronic, intramolecular, covalent-bond and hydrogen-bond subsystems. According to the symmetry $\Phi_{n1} = \Phi_{n2}$, $Q_{n1} = Q_{n2}$ and $x_{n1} = x_{n2}$, the two strands exhibit patterns of equal amplitude except for $y_{n1} = -y_{n2}$. Therefore the excitation (polaron) energy is equally shared between the two strands. As regards the excitation pattern on an individual strand, the electron is exponentially localized at the central site (see figure 2(a)). The associated pattern of the distortions of the intramolecular oscillators is exponentially localized, too. The pattern of displacements of the peptide groups in horizontal direction $x_{n\mu}$ is characterized by a kink-like shape. Accordingly, for the covalent bonds to the right (left) of the central site, the further they are from the central site, the more stretched (compressed) they become. In the vertical direction the localized amplitudes $y_{n\mu}$ have opposite signs, i.e. $y_{n,1} \geqslant 0$ and $y_{n,2} \leqslant 0$. Hence the H bonds get compressed. The peptide group at the central site has the largest amplitude of displacement from its equilibrium position and with growing distance from the central site the amplitudes of the vertical distortions decay exponentially. For the two peptide groups oppositely situated at the central sites, the degree of compression is maximal and rapidly diminishes with further

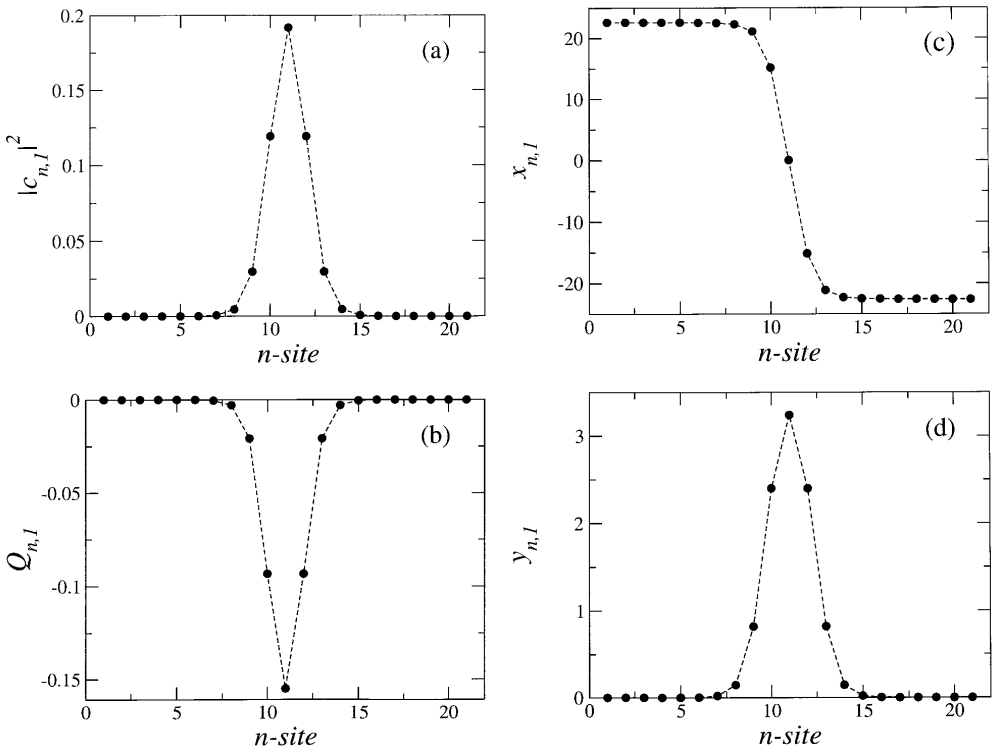

Figure 2. The two-strand ladder system. Polaron wave functions for $W = 0.4$, $D = 0.06$, $a = 0.1$, $b = d = 0.05$, $\kappa = 1.0$, $\beta_l = \beta_t = 0.001$, $\alpha = 0.001$ and $\gamma = 0.1$. In view of the symmetry, only the polaron components of the first strand are shown. (a) The electronic occupation probability $|c_{n,1}|^2$. (b) The displacements of the intramolecular coordinate $Q_{n,1}$. (c) The horizontal distortion $x_{n,1}$ of the peptide groups from their equilibrium positions. (d) The vertical distortion $y_{n,1}$ of the peptide groups from their equilibrium positions.

horizontal sepatation from these sites. Remarkably, the distortions of the peptide groups in the x-direction, i.e. along the alignment direction of the rather rigid covalent bonds, are more pronounced than those in the y-direction along which the soft H bonds are oriented. The bond deformations become stronger as the coupling parameter κ becomes larger, which is connected with a stronger electron localization.

We considered also the polaron states of extended β-sheet aggregates consisting of 21 coupled strands. The corresponding stationary excitation patterns are depicted in figure 3. The exponentially localized electronic wave function is more extended horizontally than in the vertical direction. This vertical confinement of the electron to just a few strands is due to the relatively small value of the corresponding transfer matrix element $W = 0.4$ preventing considerable vertical spreading of the electron and thus suppressing also the activation of electron motion along the hydrogen channel. Therefore we expect the electron to be more mobile in the vertical direction along the covalent channel (see the further discussion below).

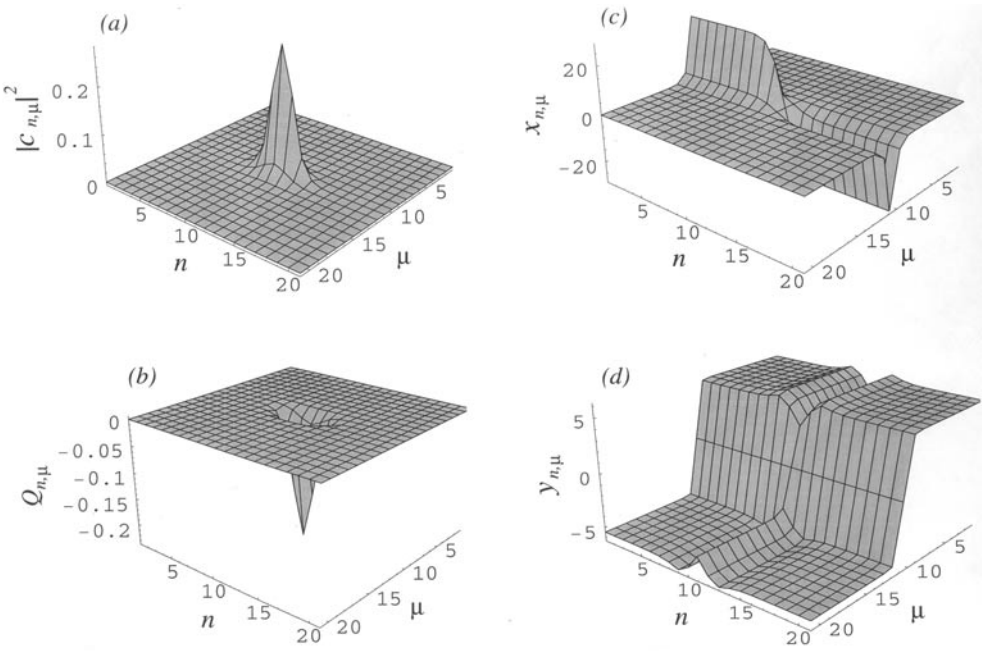

Figure 3. The polaron state on an extended β-sheet aggregate constituted for the purposes of better visualization of 21 coupled strands. Parameters: $W = 0.4$, $D = 0.06$, $a = 0.1$, $b = d = 0.04$, $\kappa = 1.0$, $\beta_l = \beta_t = 0.001$, $\alpha = 0.001$ and $\gamma = 0.1$. (a) The electronic amplitude $c_{n\mu}$. (b) Displacements of the intramolecular coordinates $Q_{n\mu}$. (c) The horizontal distortions $x_{n\mu}$ of the peptide groups. (d) The vertical distortions $y_{n\mu}$ of the peptide groups.

4. Polaron normal modes

In this section we investigate the linear stability of the polarons. Furthermore we focus attention on the existence of localized internal modes among the polaron normal modes. Such localized internal modes play a fundamental role in the formation, stability and mobility of localized states such as breathers and polarons [28–34]. We impose small perturbations on the stationary

states in the following way:

$$Q_{n\mu}(t) = Q^{(0)}_{n\mu}(t) + \delta Q_{n\mu}(t) \tag{29}$$

$$x_{n\mu}(t) = x^{(0)}_{n\mu}(t) + \delta x_{n\mu}(t) \tag{30}$$

$$y_{n\mu}(t) = y^{(0)}_{n\mu}(t) + \delta y_{n\mu}(t) \tag{31}$$

$$c_{n\mu}(t) = \left\{\Phi_{n\mu} + \delta c_{n\mu}(t)\right\} \exp\left[-\mathrm{i}\frac{E}{\tau}t\right] \tag{32}$$

where $\delta Q_{n\mu}$ and $\delta c_{n\mu}$ are small quantities. Substituting (29)–(32) into the system (11)–(15) and linearizing around ($Q_{n\mu} = Q^{(0)}_{n\mu}$, $x_{n\mu} = x^{(0)}_{n\mu}$, $y_{n\mu} = y^{(0)}_{n\mu}$, $c_{n\mu} = \Phi_{n\mu}$) gives the linear system of tangent equations which we express using the perturbation vector

$$\Delta = (\delta c_{n\mu}, \delta c^{*}_{n\mu}, \delta Q_{n\mu}, \delta \dot{Q}_{n\mu}, \delta x_{n\mu}, \delta \dot{x}_{n\mu}, \delta y_{n\mu}, \delta \dot{y}_{n\mu}) \tag{33}$$

in matrix notation:

$$\dot{\Delta} = M\Delta. \tag{34}$$

The periodic entries of the Jacobian matrix

$$M = M(\Phi_{n\mu}, \Phi^{*}_{n\mu}, Q^{(0)}_{n\mu}(t), \dot{Q}^{(0)}_{n\mu}(t), x^{(0)}_{n\mu}(t), \dot{x}^{(0)}_{n\mu}(t), y^{(0)}_{n\mu}(t), \dot{y}^{(0)}_{n\mu}(t))$$

follow from the evolution of the system (11)–(15). To analyse system (34), we proceed in a standard way using Floquet theory. We integrate the equations of motion over one period $T = 2\pi\tau/E$ to get the Floquet map

$$\Delta(T) = F\Delta(0) \tag{35}$$

giving the evolution of an initial deviation of the periodic solution after one period T with the Floquet matrix F. Linear stability of a periodic solution is ensured if all the eigenvalues $R_n \exp(\mathrm{i}\Theta_n)$ of F lie on the unit circle. Intensive numerical investigations over a wide parameter range have proved that all the polarons gained from the procedure outlined above are linearly stable.

Additionally, the Floquet analysis provides us with the frequencies of the normal modes via the relation $\omega_\Theta = \omega_e\Theta/(2\pi)$ with Θ expressed in radians. The isolated eigenvalue of the Floquet spectrum attributed to the frequency of a pinning mode is doubly degenerate, corresponding to perpendicular directions along the covalent or hydrogen bonds.

5. Polaron-assisted ET

In this section we study the mobility of polarons with the help of a numerical method originally developed for breather solutions [28]. (In fact, the electronic amplitude pattern $c_{n\mu} = \Phi_{n\mu}\exp(-\mathrm{i}Et)$ can be regarded as a static electron breather solution [29].) Following [28] we initiate the motion of polarons through suitable perturbations of the momentum variables $\{\dot{p}^{(x)}_{n\mu}\}$ targeted in the horizontal direction of the pinning mode component along the covalent bonds; that is, we use for the numerical integration of the system (11)–(15) the initial conditions

$$\left\{\Phi_{n\mu}, 0, Q^{(0)}_{n\mu}, 0, x^{(0)}_{n\mu}, 0, y^{(0)}_{n\mu}, 0\right\} + k\left\{0, 0, 0, 0, 0, \xi_{n\mu}, 0, 0\right\} \tag{36}$$

where the normalized momentum part of the pinning mode is ξ and k is the perturbation strength. Furthermore we imposed periodic boundary conditions. Due to the lattice discreteness the polarons are pinned and have to overcome a certain Peierls–Nabarro energy barrier in order to become mobile along the discrete lattice [30, 31]. Mobility is achieved for

an overcritical perturbation strength k as long as the (stationary) polaron extent is not too small [28, 35].

In figure 4 we illustrate the motion of the polaron initiated on a two-strand ladder system. The coherently moving electron (figure 4(a)) is accompanied by its localized pattern of intramolecular coordinate distortions as well as the deformation field of the horizontal and vertical displacements of the peptide groups. Note that there are (virtually) no radial losses and the polaron maintains its profile and energy content.

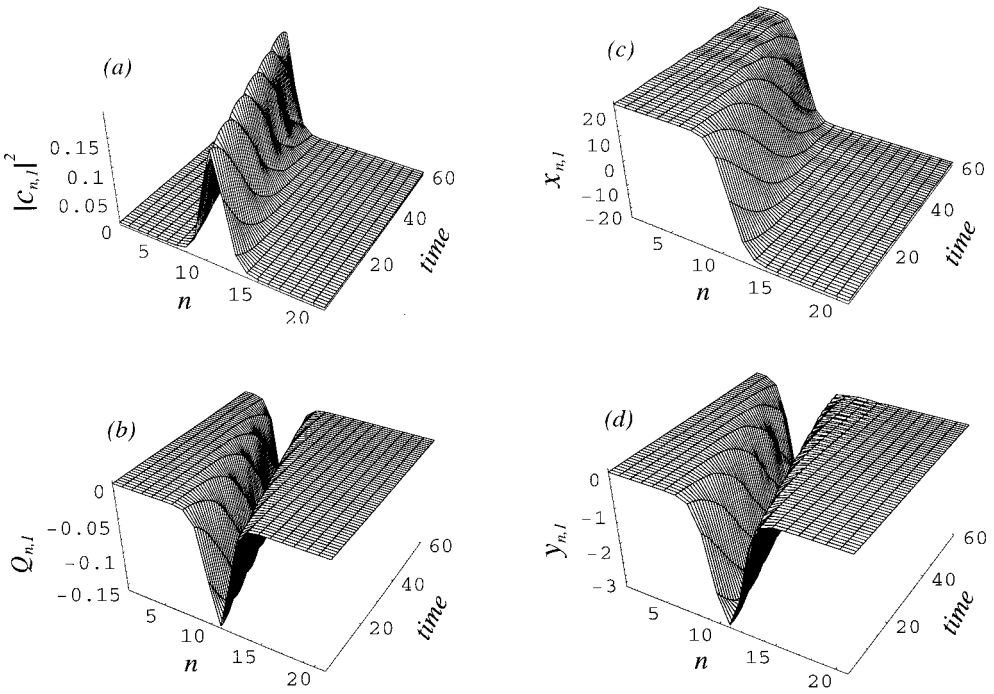

Figure 4. The moving polaron state on the two-strand ladder system. The parameters are as for figure 2 and the kicking strength is $k = 0.03$ and the time in dimensionless units is multiplied by 1000. (a) The soliton-like electronic amplitude $|c_{n,1}|$. (b) Displacements of the intramolecular coordinates $Q_{n,1}$. (c) The horizontal distortions $x_{n,1}$ of the peptide groups. (d) The vertical distortions $y_{n,1}$ of the peptide groups.

The evolved components of a mobile polaron on an extended two-dimensional β-sheet after 6000 time units are displayed in figure 5. The stationary polaron state illustrated in figure 3 provides the initial configuration which experiences a kick along the longitudinal momentum component of its pinning mode. The polaron has coherently moved over ten lattice sites across the covalent bonds. We remark that motion perpendicular to the covalent bonds, i.e. along a hydrogen path, can be accomplished also through the excitation of the corresponding vertical part of the pinning mode corresponding to the momentum variables $\{\dot{p}^{(y)}_{n\mu}\}$. However, the motion along the hydrogen channel proceeds with lower velocity than that along the covalent one.

Remarkably, although the polaron's extent is rather small (its electronic component is confined to just five sites), it is nevertheless mobile. The latter feature has to be distinguished from the properties of the polarons of the standard two-dimensional Holstein system for which only small-polaron formation is possible; however, due to their small size, these polarons

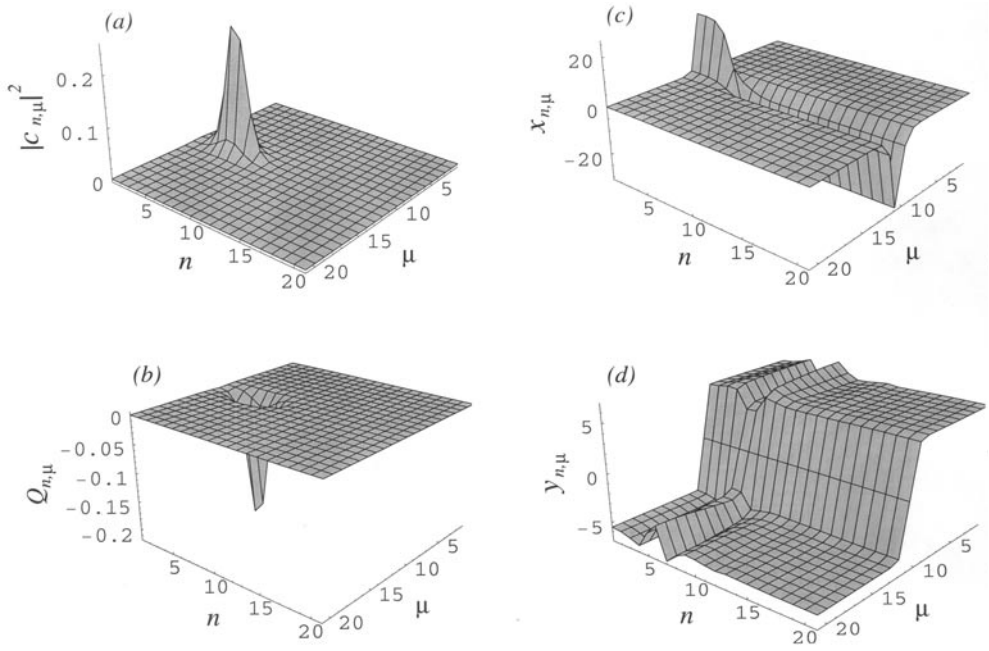

Figure 5. Mobile polarons on an extended two-dimensional β-sheet illustrating the spatio-temporal evolution of an initial polaron state depicted in figure 3 after 6000 time units. In the initial conditions the momentum component of the pinning mode targeted along the covalent bonds was included with kicking strength $k = 0.3$.

cannot propagate on the rigid lattice [24–26]. The inclusion of on-site lattice anharmonicity in the (rigid-lattice) Holstein system makes the formation of medium and large polarons also possible in two and three dimensions [27, 35, 36]. Furthermore, in the presence of non-linearity a low-frequency pinning mode vital for the activation of polaron mobility exists in all dimensions [27, 35]. Similarly, as demonstrated in this work, when the couplings of the lattice vibrations (non-rigid lattice) to the electron and the intramolecular vibrations are taken into account, uniformly propagating polarons can be constructed using a low-frequency pinning mode. This underlines the crucial role played by the bond vibrations in polaron mobility [27, 35].

6. Summary

In this paper we have considered the ET in the context of β-sheet protein models. The regular arrangement of the protein secondary structure is modelled by a two-dimensional lattice system where each site is attributed to a peptide group allowed to perform planar motions. The hydrogen-bond and covalent-bond interactions between the peptide groups are modelled via pair potentials. Each peptide group has an internal vibrational degree of freedom representing e.g. the fast amide-I mode. The motion of the electron over the peptide groups is described by a tight-binding system. The various dynamical degrees of freedom are mutually coupled, making the exchange of electronic, intramolecular and intermolecular vibrational energy possible.

We have studied the problem of stationary polarons with respect to the formation of self-trapped states. For vanishing momenta of the vibrational degrees of freedom we have been

able to derive a generalized non-linear Schrödinger equation for the electronic amplitude. Localized stationary solutions of the latter correspond then to the electronic part of the polaron. Subsequently we inferred the vibrational polaron patterns. The static localized electron is connected with a deformation of the protein backbone. In particular in the vicinity of the localized electron the bonds are pronouncedly deformed and in the horizontal direction we observe that at any site on which the maximal electron amplitude resides the covalent bonds are compressed or stretched while in the vertical direction the length of the H bonds reduces.

In the parameter range where the polarons are of large (medium) extent we have exploited a perturbation method to initiate polaron motion. To this end we have appropriatley 'kicked' the momentum component in the direction of the corresponding pinning mode. In this way coherent polaron motion is accomplished, providing stable electron transfer in β-sheets. Comparing the transport across the covalent and hydrogen channels we conclude that the former supports faster electron transfer than the latter.

This work has demonstrated that the coupling between electronic vibrational and elastic degrees of freedom in a β-sheet model can induce stable localized mobile structure. These coherent polaron structures assist ET since they effectively stabilize locally the vibrational and elastic degrees of freedom. As a result the electronic motion becomes more coherent and robust. It would be interesting to search experimentally for the role of these polarons in β-sheet configurations.

Acknowledgments

One of the authors (DH) acknowledges support by the Deutsche Forschungsgemeinschaft via a Heisenberg fellowship (He 3049/1-1) and would like to express his gratitude for the warm hospitality of the University of Crete, Heraklion, and one of the authors (NKV) gratefully acknowledges the support of the Institut für Theoretische Physik, Freie Universität Berlin. The authors are also grateful for support under the LOCNET EU network HPRN-CT-1999-00163.

References

[1] Landau L D 1933 *Z. Sowjetunion* **3** 664
[2] Pekar S I 1946 *J. Phys. (Moscow)* **10** 341
Pekar S I 1946 *J. Phys. (Moscow)* **10** 347
[3] Davydov A S 1973 *J. Theor. Biol.* **38** 559
Davydov A S and Kislukha N I 1976 *Sov. Phys.–JETP* **44** 571
Davydov A S 1982 *Sov. Phys. Rev.* B **25** 898
[4] Davydov A S 1985 *Solitons in Molecular Systems* (Dordrecht: Reidel)
Davydov A S 1973 *J. Theor. Biol.* **38** 559
[5] Christiansen P L and Scott A C (ed) 1991 *Davydov's Soliton Revisited* (New York: Plenum)
[6] Peyrard M (ed) 1995 *Nonlinear Excitations in Biomolecules (Proc. Int. School) (Les Houches, 1994)* (Berlin: Springer)
[7] Scott A C 1992 *Phys. Rep.* **217** 1
[8] Olsen O H, Samuelsen M R, Petersen S B and Nørskov L 1988 *Phys. Rev.* A **38** 5856
[9] Zolotaryuk A V, Christiansen P L and Savin A V 1996 *Phys. Rev.* E **54** 3881
[10] Christiansen P L, Zolotaryuk A V and Savin A V 1997 *Phys. Rev.* E **56** 877
[11] Zolotaryuk A V, Spatschek K H and Savin A V 1996 *Phys. Rev.* B **54** 266 and references therein
[12] Caspi S and Ben-Jacob E 1999 *Europhys. Lett.* **47** 522
[13] Englander S W, Kallenbach N R, Heeger A J, Krumhansl J A and Litwin S 1980 *Proc. Natl Acad. Sci. USA* **77** 7222
[14] Peyrard M and Bishop A R 1989 *Phys. Rev. Lett.* **62** 2755
[15] Gaeta G, Reiss C, Peyrard M and Dauxois T 1994 *Riv. Nuovo Cimento* **17** 1

[16] McCammon J A and Harvey S C 1987 *Dynamics of Proteins and Nucleic Acids* (Cambridge: Cambridge University Press)
[17] Alberts B, Bray D, Lewis J, Raff M, Roberts K and Watson J D 1983 *Molecular Biology of the Cell* (New York: Garland)
[18] Branden C and Tooze J 1991 *Introduction to Protein Structure* (New York: Garland)
[19] Schneider J P and Kelly J W 1995 *Chem. Rev.* **95** 2169
[20] Gellmann S H 1998 *Curr. Opin. Chem. Biol.* **2** 717
[21] Agegeli A *et al* 1997 *Nature* **386** 259
[22] Nyrkova I A, Semenov A N, Aggeli A and Boden N 2000 *Eur. Phys. J.* B **17** 481
[23] Yomosa S 1985 *Phys. Rev.* A **32** 1752
[24] Holstein T D 1959 *Ann. Phys., NY* **8** 325
Holstein T D 1959 *Ann. Phys., NY* **8** 343
[25] Emin D 1982 *Phys. Today* **35** 34
[26] Gerlach B and Löwen H 1991 *Rev. Mod. Phys.* **63** 63
[27] Kalosakas G, Aubry S and Tsironis G P 1998 *Phys. Rev.* B **58** 3094
[28] Chen D, Aubry S and Tsironis G P 1996 *Phys. Rev. Lett.* **77** 4776
[29] Hennig D and Tsironis G P 1999 *Phys. Rep.* **307** 333 and references therein
[30] Peyrard M and Kruskal M D 1984 *Physica* D **14** 88
[31] Flach S and Willis C R 1998 *Phys. Rep.* **295** 181
[32] Johansson M and Aubry S 1997 *Nonlinearity* **10** 1151
[33] Cretegny T and Aubry S 1997 *Phys. Rev.* B **55** 11 929
[34] Baesens C, Kim S and MacKay R S 1998 *Physica* D **113** 242
[35] Voulgarakis N K and Tsironis G P 2001 *Phys. Rev.* B **63** 14 302
[36] Zolotaryuk Y, Christiansen P L and Rasmussen J J 1998 *Phys. Rev.* B **58** 14 305